Subsecond Time-Resolved Spin Trapping Followed by Stopped-Flow EPR of Fenton Reaction Products

Jinjie Jiang,[†,§] Janet F. Bank,[†] and Charles P. Scholes*[,‡]

Contribution from the Departments of Physics and Chemistry and Center for Biochemistry and Biophysics, State University of New York at Albany, Albany, New York 12222

Received September 24, 1992

Abstract: Rapid spin-trapping kinetics on a subsecond time scale were observed from hydroxyl radicals created by the Fenton reaction where Fe(II)–EDTA and H_2O_2 were the reagents. Hydroxyl radical was trapped by the commonly used spin trap 5,5-dimethyl-1-pyrroline *N*-oxide (DMPO) to give the spin adduct DMPO-OH. The application of recent loop–gap resonator technology to stopped-flow EPR has given us the time resolution on 10-μL samples to follow rapid kinetics that were formerly only inferred from scavenger competition studies or optically monitored stopped-flow. The sub-100-ms time resolution has helped us focus straightforwardly on initial rates of trapped hydroxyl production and has put limits on any delay before radical onset. We have followed trapped hydroxyl radical production, which is completed within 1 s upon the mixing of Fe(II)–EDTA and H_2O_2 at $\sim$100 μM concentrations. The initial rate of trapped hydroxyl radical production was linearly dependent on both the initial Fe(II)–EDTA and the initial H_2O_2 concentrations. Thus, as estimated from experimental *initial* rates of DMPO-OH production, the production of hydroxyl radical that could be explicitly trapped showed a second-order reaction between Fe(II)–EDTA and H_2O_2 whose second-order rate constant was 3.2×10^3 M^{-1} s^{-1}. Beyond the first 100 ms, transient DMPO-OH formation, which indicated the availability of trappable hydroxyl radical, was limited in time. Empirical fits to the overall time course of DMPO-OH production suggested total second-order rates for the Fenton reaction of $\geq 10^4$ M^{-1} s^{-1}. An explanation for the difference between this larger rate and the smaller 3.2×10^3 M^{-1} s^{-1} rate is that the reaction yielding explicitly trapped hydroxyl radical is only one of several that consume H_2O_2 and Fe(II)–EDTA reactants. Preliminary time-resolved spin-trapping studies were done on a radical created by the Fenton reaction from ethanol to determine that the kinetic behavior of this radical does not simply parallel the production of trapped hydroxyl radical.

Introduction

Over the last decade, new technology in small microwave resonant structures has been applied to EPR.[1] The loop–gap resonator (LGR) has a much greater filling factor, a much smaller sample size, and less sensitivity to dielectric loss than a standard X-band EPR cavity.[2] To create a LGR-based, rapid-mix, stopped-flow EPR system with millisecond time resolution, Hubbell and co-workers integrated an X-band LGR having a 1.5-μL sample volume with an Update Instruments (Madison, WI) Wiskind grid mixer and RAM Driver.[3] We recently combined such a device with the methodology of spin probe oximetry.[4,5] Oxygen-dependent relaxation of a preexisting, stable nitroxide spin probe provided the means to follow submicromolar kinetic changes in oxygen concentration due to microliter quantities of cytochrome *c* oxidase at micromolar concentration, and the time resolution after stopping flow was better than 30 ms.[4,5] We now focus our LGR-based stopped-flow apparatus on following in a subsecond time regime the kinetics of a trapped radical species.

Dating from the early work of Fenton, hydrogen peroxide in the presence of ferrous ion has long been known as a strong oxidizing agent.[6a] The reaction

$$Fe(II) + H_2O_2 \rightarrow Fe(III) + HO^- + HO^\bullet \qquad (1)$$

has been proposed as a major source of reactive, short-lived, biologically toxic species, especially of HO•. In the DNA footprinting technique, Fenton reagents, where Fe(II)–EDTA was the iron chelator, have provided a useful source of DNA-damaging radicals.[6b] HO• can be identified most directly through the spin-trapping technique when spin traps such as DMPO react with HO• to give a spin-trapped adduct which is a known, well-

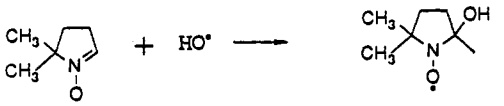

identified, generally stable nitroxide radical having a characteristic EPR signal.[7,8] Reactive radicals like the ethanol radical, which may be created as a secondary radical by oxidants arising from the Fenton reaction, also give characteristic signatures upon being trapped by DMPO.[10]

Although trapped HO• is a product of the Fenton reaction, the question exists as to whether HO•, sufficiently free to be trapped, is the initially formed oxidant or whether there may be prior formation of other intermediates.[7,10–13] Direct kinetic measure-

* To whom correspondence should be addressed.
† Department of Physics.
§ Present address: Room 601 Rensen Bldg., HB77AB, Dartmouth Medical School, Hanover, NH 03755.
‡ Department of Chemistry and Center for Biochemistry and Biophysics.

(1) Abbreviations: EPR, electron paramagnetic resonance; LGR, loop–gap resonator; i.d., inside diameter; o.d., outside diameter; ptp, peak-to-peak; HO•, hydroxyl radical; DMPO, the spin trap 5,5-dimethyl-1-pyrroline *N*-oxide; Tempo-OH, 4-hydroxy-2,2,6,6-tetramethylpiperidinyl-1-oxy; DMPO-OH, hydroxyl radical adduct of DMPO; DMPO-ET, ethanol radical adduct of DMPO; DETAPAC, diethylenetriaminepentaacetic acid; EDTA, ethylenediamine-*N*,*N*,*N*′,*N*′-tetraacetate; DTPA, diethylenetriamine-*N*,*N*,*N*′,*N*″,*N*″-pentaacetic acid; PEEK, polyether ether ketone.

(2) Froncisz, W.; Hyde, J. S. *J. Magn. Reson.* **1982**, *47*, 515–521.
(3) Hubbell, W. L.; Froncisz, W.; Hyde, J. *Rev. Sci. Instrum.* **1987**, *58*, 1879–1886.
(4) Jiang, J.; Bank, J. F.; Zhao, W.; Scholes, C. P. *Biochemistry* **1992**, *31*, 1331–1339.
(5) Jiang, J. Ph.D. Thesis, SUNY at Albany, 1992.
(6) (a) Fenton, H. J. H. *J. Chem. Soc. Trans.* **1894**, *65*, 899–910. (b) Tullius, T. *Nature* **1988**, *332*, 633.
(7) Yamazaki, I.; Piette, L. *J. Biol. Chem.* **1990**, *265*, 13589–13594.
(8) A second-order rate constant between HO• (or ethanol radical) and the DMPO spin trap of the order of 10^9 M^{-1} s^{-1} has been estimated from photolysis experiments (ref 9), and such a large rate constant would ensure that the reaction of HO• radical with the spin trap, if it is like HO• created by photolysis, is not a rate-limiting step in our studies.
(9) Finkelstein, E.; Rosen, G. M.; Rauckman, E. J. *J. Am. Chem. Soc.* **1980**, *102*, 4994–4999.
(10) Yamazaki, I.; Piette, L. *J. Am. Chem. Soc.* **1991**, *113*, 7588–7593.
(11) Rush, J. D.; Koppenol, W. H. *J. Biol. Chem.* **1986**, *261*, 6730–6733.

0002-7863/93/1515-4742$04.00/0

ment of trapped radicals can identify HO• and provide information on initial rates of its formation, on time lags or delays in trapped HO• production, and on overall kinetics of trapped HO• production. Much previous work based on stoichiometric[14] or kinetic analyses and scavenger perturbation upon the amount of final products[13] has not directly probed for highly reactive hydroxyl intermediates in the way that spin trapping can. In most spin-trapping experiments carried out with standard EPR apparatus, the analysis of spin-trapped radical has been done long after the fact of radical production. The recent work of Yamazaki and Piette[7,10] stands out in showing the utility and feasibility of kinetic measurements for spin trapping, albeit in that study the kinetics were done with systems like the DETAPAC-coordinated Fenton system that slowly evolved trapped HO• on an ~10–s time scale and with a standard EPR cavity and flow-flat cell[15] stopped-flow system appearing to have inherently low time resolution. No subsecond kinetic measurements were reported.[7,10] Judging from our experience in preliminary oximetry measurements, the flow-flat cell system in a stopped-flow configuration is highly vibration-sensitive, will use approximately milliliter quantities per shot, and will not readily adapt to subsecond kinetic measurements.[16] If one has copious amounts of inexpensive reactants, a continuous-flow system can provide information on transient species[17,18] as they exist at discrete times after mixing if the dead volume between mixing and observation is well defined.[19] A recently reported flow study used 2.5 mL s^{-1} to obtain a time of 27 ms between mixing and observation.[18] (Stopped-flow would show the continuous time evolution of such species.)

Fe(II)–EDTA has been an especially common Fenton reagent,[6b,11] and the rapid time course of trapped HO• production occurs over about 1 s when initial Fe(II)–EDTA and H_2O_2 reagent concentrations are of the order of 100 μM. Such reagent concentrations are those commonly used for optical stopped-flow monitoring of oxidation of Fe(II)–EDTA by H_2O_2.[11] However, until the advent of the LGR stopped-flow system, concomitant stopped-flow EPR measurements had not been feasible under the reagent conditions and time constraints used for optical stopped-flow.

Experimental Section

Methods. Modifications to the Bruker EPR spectrometer, the EPR software package (Scientific Sales Systems, Bloomington, IL), and the details of the LGR-based EPR stopped-flow system are described elsewhere.[4,5] The sample with approximately 1.5 μL of active volume is contained in a 0.6-mm i.d., 0.8-mm o.d. quartz tube that extends through the LGR from the mixer about 1 cm below the LGR. The sensitivity of the LGR containing a nitroxide sample in this tube is ~30 times larger than that of the standard X-band cavity containing the same small sample. If one has plentiful sample, then an X-band liquid flat cell containing ~100 μL of active volume in a standard X-band TE_{102} cavity will give about 50% more sensitivity than the 1.5-μL sample in the LGR. The effective dead time following mixing, which includes the 15-ms braking time for the RAM, was 18 ms.[4] A major development aspect of the work in refs 4 and 5 was to understand and minimize artifacts (transient overshoots, undershoots, and "glitches") that could occur after flow was stopped.[20] For the present experiments, new PEEK syringe plungers replaced stainless steel plungers, which were formerly the major metal objects contacting the sample in the storage syringe. The transfer lines from syringes to the mixer were high-pressure (HPLC) 0.02-in. i.d. PEEK tubing. All work was carried out at ambient temperature of 21 ± 1 °C.

For obtaining initial rates of trapped spin buildup and for fitting overall kinetic behavior to kinetic schemes, the ASYSTANT (Macmillen Software Co., New York) data analysis program was applied to digitally collected EPR data.

Materials. DETAPAC, EDTA, DMPO, and Tempo-OH were obtained from Sigma. The stable Tempo-OH nitroxide radical was needed for spin quantitation, and for Tempo-OH we measured and used an extinction coefficient of 1.44 mM^{-1} cm^{-1} at 240 nm.[21a] DMPO was stored under argon atmosphere at –20 °C until aliquots were withdrawn by gas-tight syringe before an experiment. Glass-distilled water was used throughout. Hydrogen peroxide solutions were prepared before every experiment from a 30% hydrogen peroxide stock solution whose concentration had been determined from the absorbance of I_3^- (ϵ_{353} = 2.55×10^4 M^{-1} cm^{-1}) which is formed in the molybdate-catalyzed oxidation of potassium iodide.[21b] As in the work of refs 7 and 10, an A solution was prepared in aerobic buffer which contained 150 mM KCl, 40 mM potassium phosphate buffer (pH 7.4), 40 mM DMPO, 400 μM chelator, H_2O_2, and an O_2 concentration that was about 200 μM. The ferrous ion solution (solution B) was prepared before every experiment by dissolving ferrous ammonium sulfate ($Fe(NH_4)_2(SO_4)_2 \cdot 6H_2O$) with no chelator in anaerobic, argon-purged 150 mM KCl solution and then anaerobically transferring the solution to a gas-tight syringe. Reactions were initiated by mixing equal volumes of solutions A and B so that after mixing the concentrations of all compounds except KCl was half of their starting concentrations. (Ferrous ion concentration after mixing was always kept at less than half of the chelator concentration.) Reference 10 indicated that for trapping HO• created by an Fe(II)–EDTA Fenton system, the DMPO concentration was about 90% saturated at 20 mM DMPO. Experiments to probe for ethanol-oxidizing species were generally carried out with ethanol at 1.65 M concentration in both A and B syringes.

Results

Figures 1A and 1B, respectively, show characteristic signals from spin-trapped DMPO-OH and DMPO-ET radicals. For kinetic measurements, we placed the magnetic field at position a for DMPO-OH radical and at position b for the DMPO-ET radical. Positions a and b do not overlap. In our quantitation procedure for spin-trapped radicals, we first doubly integrated the EPR spectrum of the spin-trapped species, as obtained at a nonsaturating microwave power and with a field modulation less than the natural line width. To estimate the concentration of trapped radical, we then compared the doubly integrated spectrum of the trapped spin with the doubly integrated spectrum of the stable Tempo-OH radical of known concentration. Next, at a known gain setting, we calibrated the field-modulated EPR signal height of the kinetically monitored peak in Figure 1 versus the integrated number of trapped spins to relate that height to the underlying trapped-spin concentration. From repeated measurements, we estimate a ±20% uncertainty in relating the field-modulated EPR signal height of the kinetically monitored peak to underlying trapped-signal concentration.

Experimental traces of spin-trapping kinetics are shown in Figure 2. The conditions of Figure 2A were those from a Fenton reagent where DETAPAC was an Fe(II) chelator and trapped HO• was slowly but efficiently produced.[7,10] Subsecond kinetics in Figure 2B occurred where more commonly used EDTA was the Fe(II) chelator and the respective Fe(II)–EDTA and H_2O_2 concentrations were 100 and 600 μM. For Figure 2B, a rapid-mix, stopped-flow system was necessary both for determining the initial reaction rate and for resolving the overall detailed transient

(12) Rush, J. D.; Koppenol, W. H. *J. Inorg. Biochem.* **1987**, *29*, 199–215.
(13) Rahhal, S.; Richter, H. W. *J. Am. Chem. Soc.* **1988**, *110*, 3126–3133.
(14) Walling, C. *Acc. Chem. Res.* **1975**, *8*, 125–131.
(15) Yamazaki, I.; Mason, H. S.; Piette, L. *J. Biol. Chem.* **1960**, *235*, 2444–2449.
(16) Scholes, C. P.; Bank, J. F.; Fan, C.; Taylor, H. In *Advances in Membrane Biochemistry and Bioenergetics*; Kim, C. H., Ed.; Plenum Press: New York, 1987; pp 439–447.
(17) Shiga, T. *J. Phys. Chem.* **1965**, *69*, 3805–3814.
(18) Croft, S.; Gilbert, B. C.; Lindsay Smith, J. R.; Stell, J. K.; Sanderson, W. R. *J. Chem. Soc., Perkin Trans. 2* **1992**, 153–160.
(19) Flow through the X-band flow-flat cell is not uniform, and the liquid near the outside edges of the flat region does not readily flush from the cell. (Madden, K. M., personal communication.)
(20) In refs 4 and 5, experiments were done to measure the transient destruction of a spin probe by high levels of ascorbate over a few hundred milliseconds after mixing, thus repeating similar experiments of ref 3. These experiments showed that the LGR system can measure rapid kinetics at times considerably less than 100 ms after mixing. In the course of spin probe oximetry experiments where we were observing change in a large preexisting probe signal, we reduced obscuring transient artifacts to times less than 30 ms after mixing and to heights less than 20 mV.
(21) (a) Morrisett, J. D. In *Spin Labelling, Theory and Applications*; Berliner, L. J., Ed.; Academic Press: New York, 1976; pp 274–338. (b) Cotton, M. L.; Dunford, H. B. *Can. J. Chem.* **1973**, *51*, 582–586.

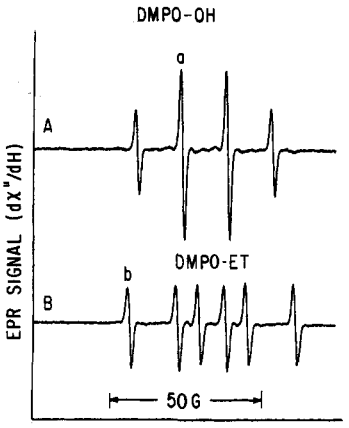

Figure 1. (A) Spectrum of spin-trapped DMPO-OH taken approximately 1 min after flow stopped. The solutions were mixed as described in the Experimental Section, and the concentration of reactants just after mixing was 150 mM KCl, 20 mM pH 7.4 phosphate buffer, 20 mM DMPO, 100 μM Fe(II), 200 μM EDTA, and 600 μM H_2O_2. This spectrum was obtained with a modulation of 1.25 G ptp, time constant 20 ms, gain of 1.25×10^4, EPR frequency of 9.456 GHz, and microwave power of 2 mW. Position a shows the feature which was kinetically monitored in stopped-flow experiments. Our calibration procedure indicated that this spectrum contained a concentration of 25 μM DMPO-OH. (B) Spectrum of spin-trapped DMPO-ET taken approximately 1 min after flow stopped. Reactants were as in A except that the solution after mixing contained 1.65 M ethanol. Feature b was kinetically monitored in stopped-flow experiments. The spectrum was obtained with the EPR conditions of A. Our calibration procedure indicated that this spectrum contained a concentration of 28 μM DMPO-ET.

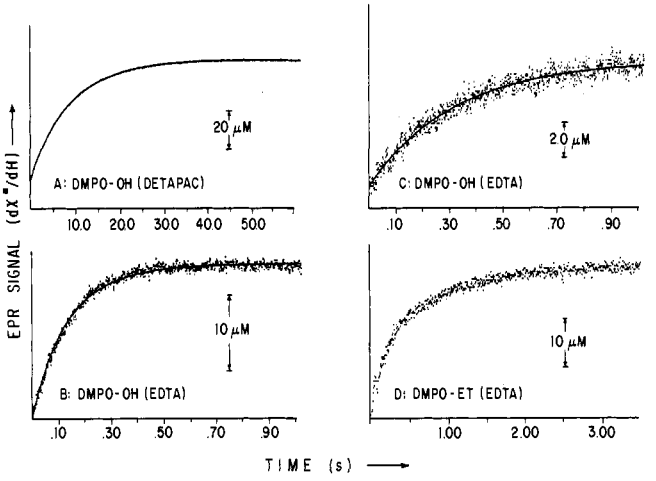

Figure 2. Kinetic transients obtained by spin trapping. (A) Time-resolved spin-trapped HO• from DMPO-OH as it appeared over 60 s when DETAPAC was the Fe(II) chelator; time constant, 20 ms. The solution conditions after mixing were 150 mM KCl, 20 mM pH 7.4 phosphate buffer, 20 mM DMPO, 100 μM Fe(II), 200 μM DETAPAC, and 600 μM H_2O_2. (B) Time-resolved spin-trapped HO• from DMPO-OH as it appeared over 1.0 s when EDTA was the Fe(II) chelator; time constant, 1 ms. Solution conditions identical to those of A except 200 μM EDTA instead of DETAPAC was the chelator. The underlying fit described in the Discussion yielded $k_{tot} = 1.3 \times 10^4$ M^{-1} s^{-1} and $f = 0.21$. (C) Time-resolved spin-trapped HO• from DMPO-OH as it appeared over 1.0 s when EDTA was the Fe(II) chelator but with a smaller concentratin of Fe(II) than in B; initial Fe(II) concentration was 67 μM and H_2O_2 concentration was 200 μM. The underlying fit yielded $k_{tot} = 1.6 \times 10^4$ M^{-1} s^{-1} and $f = 0.23$. (D) Time-resolved spin-trapped ethanol radical from DMPO-ET as it appeared over *3.5 s* when EDTA was the Fe(II) chelator. Concentrations of reactants were as in B except that the solution contained 1.65 M ethanol.

shape, which could be later fit to a kinetic model. The superimposed fit in Figure 2B is to a second-order reaction scheme, whose approximate nature is discussed below.[28,29] The DMPO-OH signal increased linearly over at least the first 100 ms so that an initial rate could readily be determined, independent of an assumed reaction scheme. If there is a delay in the onset of a linear DMPO-OH signal increase (due, for example, to production of a transient predecessor to trapped HO•), we estimate within the noise of Figure 2B that this delay is ≤20 ms. The 0.02-s upper limit on a delay in producing trapped DMPO-OH is a time limit newly delineated by our stopped-flow spin-trapping measurements.

The spin-trapping kinetics of Figure 2C were obtained with lower concentrations of Fe(II)–EDTA and H_2O_2 than those in Figure 2B. Even though the overall amount of trapped signal was small and the time course of Figure 2C was rapid, it was still possible to follow the kinetic behavior and to estimate the initial reaction rate. We noticed that if an excess of Fe(II)–EDTA was mixed with H_2O_2, a slow decay of spin-trapped DMPO-OH radical set in following the initial rapid creation of DMPO-OH. It has been suggested that Fe(II)–EDTA will reduce DMPO-OH.[7] This slow decay did not interfere with measuring the initial rate of DMPO-OH production over the first few hundred milliseconds, and for all but the lowest H_2O_2 concentrations (10 or 33 μM H_2O_2 vs 100 μM Fe(II)–EDTA) the slow decay did not set in until the overall kinetic time course of DMPO-OH buildup was complete.

Ethanol will react not only with HO• but conceivably with other suggested Fenton oxidants (e.g., hypervalent iron or bound HO•) to produce a trapped ethanol radical.[7,10] Therefore we compared the kinetic behavior of trapped DMPO-ET with the behavior of the trapped DMPO-OH under conditions where the kinetic behavior was initiated by mixing the same concentrations of Fe(II)–EDTA and H_2O_2. A comparison of Figure 2B (DMPO-OH kinetics on a 1-s total time scale) and Figure 2D (DMPO-ET kinetics on a 3.5-s total time scale) shows that buildup of DMPO-ET radical takes longer than that of DMPO-OH. The half-time for reaction is ~300 ms for DMPO-ET vs ~100 ms for DMPO-OH. The field position for measuring DMPO-ET was different from that for DMPO-OH so that we were not simultaneously monitoring the buildup of DMPO-ET and DMPO-OH at the same magnetic field. The experimental trace for DMPO-ET did not consist of a fast transient like that of DMPO-OH followed by a slower transient. The obvious difference in our kinetics between DMPO-OH and DMPO-ET is evidence that production of DMPO-ET is due to additional reactive species beyond those that yield spin-trapped HO•. Flow studies have shown that Fenton chemistry of ethanol, (no spin trap present) yields both α-carbon and β-carbon radicals of ethanol[17,18] and that the α radical may react with the Fe(III)–EDTA.[18] Since the α radical of ethanol is also what reacts with DMPO to yield DMPO-ET,[10] we believe that the Fenton system with ethanol added is sufficiently complex to merit a separate future study.

Discussion

Our kinetic traces gave us the time resolution to measure initial reaction rates from the linear increase of DMPO-OH. Since we could measure initial rates of explicitly trapped HO• production and its explicit dependence on initial concentrations of H_2O_2 and Fe(II)–EDTA, we were less sensitive to complications from stoichiometry and mechanism that become progressively more important[13] in determining the kinetics as the reaction proceeds. These initial rates were quantitatively determined by fitting the digital EPR data to a power series in time and obtaining from the power series the linear term which predominated over at least the first 100 ms. Figure 3A shows initial rates of trapped HO• production plotted as a function of starting Fe(II)–EDTA concentration (called $[Fe(II)]_0$) over a >1 order of magnitude range (3–100 μM) as the initial peroxide concentration (called $[H_2O_2]_0$) was being held constant at 200 μM. Figure 3B shows the initial rates of trapped HO• production plotted as a function

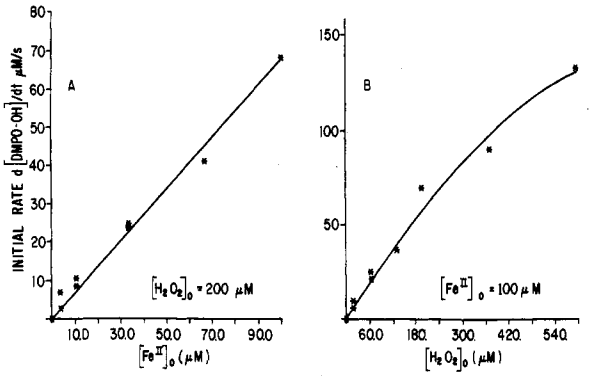

Figure 3. (A) Plot of initial rate of DMPO-OH production as a function of initial Fe(II)–EDTA concentration with $[H_2O]_0 = 200\ \mu M$ as taken from the linear region of DMPO-OH build up. The solid line is the least-squares-fitted line to the expression $d[DMPO\text{-}OH]/dt = A[Fe(II)]_0$, where $A = 0.65 \pm 0.02\ s^{-1}$. The term in A gave $k_{HO} = (3.3 \pm 0.2) \times 10^3\ M^{-1}s^{-1}$. (B) Plot of initial rate of DMPO-OH production as a function of initial $[H_2O_2]_0$ concentration with $[Fe(II)]_0 = 100\ \mu M$. The solid line is the least-squares-fitted line to the expression $d[DMPO\text{-}OH]/dt = A[H_2O_2]_0 + B[H_2O_2]_0^2$, where $A = 0.31 \pm 0.02\ s^{-1}$ and $B = (-1.8 \pm 0.5) \times 10^{-4}\ \mu M^{-1}\ s^{-1}$. The term in A gave $k_{HO} = (3.1 \pm 0.2) \times 10^3\ M^{-1}\ s^{-1}$.

of $[H_2O_2]_0$ over a 2 order of magnitude range (20–600 μM) as $[Fe(II)]_0$ was being held constant at 100 μM. Both Figures 3A and 3B exhibited a definite linear dependence of rate on the concentration of that reactant which was being varied, although Figure 3B indicated a slight diminishment from linear behavior at highest $[H_2O_2]_0$. As determined by least-squares fitting to equally weighted points, the slope of Figure 3A, where $[H_2O_2]_0$ was held constant, was $0.65 \pm 0.02\ s^{-1}$, and the initial slope of Figure 3B, where $[Fe(II)]_0$ was held constant, was $0.31 \pm 0.02\ s^{-1}$.[22]

Since the plots in Figures 3A and 3B, respectively, showed linear dependence on $[Fe(II)]_0$ when $[H_2O_2]_0$ was held constant and on $[H_2O_2]_0$ when $[Fe(II)]_0$ was held constant, we were unambiguously led by experiment to interpret the plots in Figures 3A and 3B by a second-order bimolecular reaction scheme in which Fe(II)–EDTA and H_2O_2 react to produce HO• that can be trapped. We indicate this bimolecular step as:

$$\text{Fe(II)–EDTA} + H_2O_2 \xrightarrow{k_{HO}} \text{(trapped) HO}^\bullet \qquad (2)$$

where k_{HO} is the second-order rate constant for that component of the Fenton reagent (reaction 1) which produces the HO• that is trapped by DMPO. The initial rate for production of trapped HO• is $k_{HO}[Fe(II)]_0[H_2O_2]_0$. The slope of Figure 3A should be $k_{HO}[H_2O_2]_0$, and the slope of Figure 3B should be $k_{HO}[Fe(II)]_0$. A value of $k_{HO} = (3.3 \pm 0.2) \times 10^3\ M^{-1}\ s^{-1}$ was obtained from Figure 3A and of $k_{HO} = (3.1 \pm 0.2) \times 10^3\ M^{-1}\ s^{-1}$ from Figure 3B. Within experimental error these values of k_{HO} from both slopes are equal.[22]

HO• is an oxidizing intermediate in the Fenton reaction, and our technique is suited for measuring its time behavior. There is question whether there are even earlier rapidly formed intermediates, proposed to explain the product results in refs 7 and 10, which proceed to yield trapped HO•. These intermediates could yield DMPO-OH either by releasing HO•, which is then rapidly trapped as DMPO-OH, or by directly reacting with DMPO.[23] An advantage of kinetic spin-trapping experiments under the conditions shown in Figures 2B and 2C is that they have put a ≤20-ms time limit on the delay needed to form a putative intermediate leading to trapped HO•.[24] Another kinetic aspect of an intermediate prior to trapped HO• could be saturation kinetics if the intermediate [such as a Fe(II)–EDTA/H_2O_2 adduct][10] is in rapid equilibrium with H_2O_2 and Fe(II)–EDTA reactants and proceeds to yield trapped HO•. The fall-off from linear increase of reaction rate at the highest $[H_2O_2]_0$ in Figure 3B could imply the onset of saturation in the population of such an intermediate prior to trapping of HO•. However, we have concern that a side reaction such as destruction of an EDTA chelator[25] could cause a fall-off in rate of trapped HO• production at high $[H_2O_2]_0$ and thus mimick saturation kinetics. To probe for intermediates prior to trapped HO•, more complete stopped-flow rapid spin-trapping studies will be focused on delineating time lags and saturation kinetics.

The initial rate of DMPO-OH production can be directly measured and related to initial concentrations of available H_2O_2 and Fe(II)–EDTA. The linear behavior of this rate with $[H_2O_2]_0$ and $[Fe(II)]_0$ over a wide range of concentrations implies that k_{HO} is a *constant* independent of $[H_2O_2]_0$ and $[Fe(II)]_0$. There is information as well in the overall transient time course of DMPO-OH production which tells of the time regime when HO• is available to be trapped and of the total amount of trapped DMPO-OH. In examining the overall transient DMPO-OH production extending beyond the first 100 ms, we determined the following. First, this transient occurred over a shorter time span than would be expected just from the second-order reaction rate, $k_{HO} = 3.2 \times 10^3\ M^{-1}\ s^{-1}$, for DMPO-OH production. [For example, when we considered the case of Figure 2B where $[H_2O_2]_0 = 6[Fe(II)]_0$, the behavior of the transient, which is approximately of the form $\{1 - \exp(-(k_{tot}[H_2O_2]t)\}$, would give $k_{tot} \geq 10^4\ M^{-1}\ s^{-1} > k_{HO}$.] Second, the total concentration of trapped DMPO-OH in Figure 2B was about 20% of the initial Fe(II)–EDTA concentration, whereas, if the Fenton reaction were a simple second-order reaction producing a trapped HO• for each Fe(II)–EDTA consumed, we might have naïvely expected the DMPO-OH concentration to be 100% of the initial Fe(II)–EDTA concentration.

We realized that the overall time course of EPR-detected DMPO-OH production only indirectly reports the reactant (H_2O_2 and Fe(II)–EDTA) consumption and that EPR-detected DMPO-OH need not directly tell of other nontrapped oxidants which may be created simultaneously with trappable HO• (perhaps even from a common precursor intermediate[10]). Two such oxidants are hypervalent iron[26] and caged or confined HO•,[10] whose relative abundances compared to trappable HO• depend on the Fe(II) chelator.[27] We did not want to assume a variety of complicated steps and intermediates. Rather, to approximate and fit the time course of DMPO-OH production, we assumed a second-order reaction between Fe(II)–EDTA and H_2O_2 for which there were two phenomenological parameters to be determined. (See footnotes 28 and 29 for details.) The first parameter was k_{tot}, which might be considered as the total second-order rate constant for the Fe(II)–EDTA and H_2O_2 reaction. The second parameter was f, the fraction of reactant channeled by the second-order

(22) (a) The errors quoted in the text are from the least-squares fitting routine of Bevington (ref 22b); we suspect that the errors should additionally reflect the ±20% uncertainty in spin quantitation. Thus errors would be increased as follows: 1) For the slope of Figure 3A the error would be ±0.13 s^{-1} and the error in the value of k_{HO} computed from this slope would be ±0.6 × $10^3\ M^{-1}\ s^{-1}$. 2) For the initial slope of Figure 3A the error would be ±0.06 s^{-1} and the error in the value of k_{HO} computed from this slope would be ±0.6 × $10^3\ M^{-1}\ s^{-1}$. (b) Bevington, P. R. *Data Reduction and Error Analysis for the Physical Sciences*; McGraw Hill: New York, 1969; pp 134–163.

(23) We are grateful to a referee for pointing out this latter possibility of direct interaction between an intermediate and DMPO.

(24) If one supposes that a second-order reaction between Fe(II)–EDTA and H_2O_2 produces such a prior intermediate within 0.02 s, then when $[H_2O_2]_0 > [Fe(II)]$ and $[H_2O_2] = 600\ \mu M$ as in Figure 2B, the second-order rate constant for the production of such a prior intermediate would be $>8 \times 10^5\ M^{-1}\ s^{-1} = [(6 \times 10^{-4}\ M \times 0.02\ s]^{-1}$.

(25) Rush, J. D.; Koppenol, W. H. *J. Am. Chem. Soc.* **1988**, *110*, 4957–4963.

(26) Rush, J. D.; Maskos, Z.; Koppenol, W. H. *Methods Enzymol.* **1990**, *186*, 148–156.

(27) In a study of the Fenton oxidation of deuterated organic substrates, nonfree HO•, whose confinement depends on the nature of the Fe(II) chelator, may cause chelator-dependent kinetic isotope effects. Tang, H. C.; Kang, D.; Sawyer, D. T. *J. Am. Chem. Soc.* **1992**, *114*, 3445–3455.

reaction into trapped HO• in the form of DMPO-OH. There is thus the implicit assumption in this approach that the reaction yielding trapped HO• is only one of several second-order reactions contributing to k_{tot}. k_{HO}, k_{tot}, and f might be straightforwardly related if k_{HO} were one of several parallel second-order rates contributing to k_{tot}; then f would equal k_{HO}/k_{tot} (a relation which does approximately hold for the values of f, k_{HO}, and k_{tot} relevant to Figures 2B and 2C). A figure showing the variation of k_{tot} and f with the ratio of $[H_2O_2]_0/[Fe(II)]_0$ is in the supplementary material.

From the fitting procedure we found that when $[H_2O_2]_0 \gg [Fe(II)]_0$, k_{tot} tended to 10^4 M^{-1} s^{-1} and f became at least as large as 0.5. This value of k_{tot} is comparable with second-order rate constants (of the order of 7×10^3 M^{-1} s^{-1}) for the Fenton reaction as measured at high ratios of H_2O_2 to Fe(II)–EDTA.[26] Such second-order rate constants were obtained by observing consumption of Fe(II)–EDTA and production of Fe(III)–EDTA[12,26], or somewhat indirectly, either by using a Fenton recycling system containing paraquat radical[30] or by doing a steady-state analysis of *tert*-butyl alcohol's radical EPR signal in conjunction with continuous flow.[18,31] As the ratio of $[Fe(II)]_0/[H_2O_2]_0$ increased in our experiments, we discovered that k_{tot} increased to $\sim 10^5$ M^{-1} s^{-1} while f fell below 0.1. At high ratios of $[Fe(II)]_0$ to $[H_2O_2]_0$, an increase in the number of reaction paths yielding nonoxidizing species and a concomitant decrease in the efficiency of hydroxyl radical production have previously been reported.[7] It is encouraging that the parameters k_{tot} and f from our simple-fitting procedure have a correlation with the findings of others. Still, it must be pointed out that the second-order reaction[28] used for fitting them had to be approximate because k_{tot} and f were not constants independent of $[H_2O_2]_0$ and $[Fe(II)]_0$ over the entire range of concentrations studied.

Conclusions

Our present work shows that recent LGR-based stopped-flow technology[3-5] can be integrated with the widely used spin-trapping methodology[32] to provide sub-100-ms kinetic measurements of spin-trapped Fenton products at micromolar concentrations and in microliter sample volumes. The result is that rapid *initial* rates and rapid overall transient kinetics of radical production are readily resolved, thus opening a new possibility for EPR spin-trap studies.

Acknowledgment. This work was supported in part by NIH Grant GM 35103. Acknowledgement is made to the donors of the Petroleum Research Fund, administered by the American Chemical Society, for partial support of this research [PRF Grant No. 26117-AC4]. We are grateful to Dr. Andrzej Sienkiewicz and Mr. Ray Hansen for frequent technical advice on the LGR system.

Supplementary Material Available: Figure showing the variation of k_{tot} and of f as a function of the ratio $[H_2O_2]_0/[Fe(II)]_0$ and an accompanying figure legend (2 pages). Ordering information is given on any current masthead page.

(28) Our fit to the overall time course for DMPO-OH production was to a simplified Fenton reaction presented as a second-order reaction:

$$\text{Fe(II)–EDTA} + H_2O_2 \xrightarrow{k_{tot}} X$$

where k_{tot} is the overall rate constant for the second-order reaction and X is the extent of the reaction. Formally, $X(t)$ would be the concentration of H_2O_2 and Fe(II)–EDTA which has been consumed at time t to produce products of the second-order reaction. The fraction f is the fraction of X which is channeled into trapped HO•.

(29) The general solution to the second-order reaction of footnote 28 (above) is:

$$X(t) = [Fe(II)_0][H_2O_2]_0[1 - \exp\{k_{tot}t([Fe(II)]_0 - [H_2O_2)_0)\}]/ [H_2O_2]_0 - [Fe(II)]_0\exp\{k_{tot}t([Fe(II)]_0 - [H_2O_2]_0)\}$$

where DMPO-OH $(t) = fX(t)$.

If $[H_2O_2]_0 \gg [Fe(II)]_0$, this expression for $X(t)$ has a pseudo-first-order form:

$$X(t) = [Fe(II)]_0[1 - \exp\text{-}(k_{tot}[H_2O_2]_0t)]$$

(30) Sutton, H. C.; Winterbourn, C. C. *Arch. Biochem. Biophys.* **1984**, *235*, 106–115.

(31) Croft, S.; Gilbert, B. C.; Lindsay Smith, J. R.; Whitwood, A. C. *Free Rad. Res. Commun.* **1992**, *17*, 21–39.

(32) Janzen, E. G.; Haire, D. L. *Two Decades of Spin Trapping*; JAI Press, Inc.: Greenwich, CT, 1990; pp 253–295.